

Liquid-Phase Exfoliation of Graphite Towards Solubilized Graphenes**

Athanasios B. Bourlinos,* Vasilios Georgakilas,* Radek Zboril, Theodore A. Steriotis, and Athanasios K. Stubos

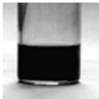
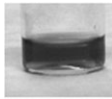

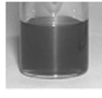
Following the astonishing discoveries of fullerenes and carbon nanotubes in earlier decades, the rise of graphene has recently triggered an exciting new area in the field of carbon nanoscience with continuously growing academic and technological impetus.^[1,2] Currently, several methods have been proposed to prepare graphenes, such as micromechanical cleavage,^[1,2] thermal annealing of SiC,^[3] chemical reduction of graphite oxide,^[4–6] intercalative expansion of graphite,^[7,8] bottom-up growth,^[9] chemical vapor deposition,^[10] and liquid-phase exfoliation.^[11] Especially this latter top-down approach is very appealing from a chemist's point of view for the following reasons: i) it is direct, simple, and benign producing graphenes just by solvent treatment of graphite powders, and ii) the as-obtained sheets form colloidal dispersions in the solvents used for the exfoliation, thereby enabling their manipulation into various processes, like mixing, blending, casting, impregnation, spin-coating, or functionalization.^[11–13] The key parameter for suitable solvents is that the solvent–graphene interactions must be at least comparable to those existing between the stacked graphenes in graphite. To that end, Coleman and coworkers have successfully demonstrated this concept using *N*-methylpyrrolidone, *N,N*-dimethylacetamide, γ -butyrolactone, 1,3-dimethyl-2-imidazolidinone, and benzyl benzoate as

solvents.^[11a] Undoubtedly, the exploration of additional solvents in this context is highly recommended in order to strengthen the universal character of this genuine approach by providing more choices.

Before the dissemination of these intriguing results by Coleman's group and driven by our background on a range of swellable layered solids (nanoclays, graphite oxide), we had been working independently for some time on the production of solubilized graphenes through solvent etching of graphite. As some of our previous attempts in this direction were discouraging, the preceding work by Coleman and coworkers timely urged us to continue our search efforts for alternative options. Herein we demonstrate a neoteric set of solvents for the liquid-phase exfoliation of graphite towards solubilized graphenes. The proposed solvents belong to a peculiar class of perfluorinated aromatic molecules^[14–16] and include hexafluorobenzene (C_6F_6), octafluorotoluene ($C_6F_5CF_3$), pentafluorobenzonitrile (C_6F_5CN), and pentafluoropyridine (C_5F_5N). Complementary to these liquids, blank experiments with the related hydrocarbon analogues unexpectedly led us to the notable case of pyridine, which is thereafter discussed separately. Along with these solvents, which are the main focus of this contribution, an assortment of other suitable dispersing media is cited in parallel. The conversion of the as-derived single sheets into metal–graphene hybrids is also presented. Overall, our results build upon the recent work of Coleman and coworkers by expanding the library of available exfoliating solvents with new members.

Graphite fine powder was suspended by sonication (1 h) in a series of perfluorinated aromatic solvents to afford moderately dark-gray colloidal dispersions (Table 1). The Tyndall effect is often used as a measure of the existence of a colloid. This light scattering effect is clearly shown for the pentafluorobenzonitrile colloid after settling (0.1 mg mL^{-1}) using the beam of a laser pointer and the optical spectrum of the corresponding dispersion after proper dilution with dimethylformamide (DMF, $10 \mu\text{g mL}^{-1}$) is also displayed

Table 1. Colloidal dispersions obtained after liquid-phase exfoliation of graphite using the perfluorinated aromatic solvents below.

Solvent	C_6F_6	$C_6F_5CF_3$	C_6F_5CN	C_5F_5N
Graphite				

[*] Dr. A. B. Bourlinos, Dr. V. Georgakilas
Institute of Materials Science, NCSR “Demokritos”
Ag. Paraskevi Attikis, Athens 15310 (Greece)
E-mail: bourlinos@ims.demokritos.gr
georgaki@ims.demokritos.gr

Prof. R. Zboril
Department of Physical Chemistry, Palacky University
Svobody 26, Olomouc 77146 (Czech Republic)

Dr. T. A. Steriotis
Institute of Physical Chemistry, NCSR “Demokritos”
Ag. Paraskevi Attikis, Athens 15310 (Greece)

Dr. A. K. Stubos
Institute of Nuclear Technology and Radiation Protection
Environmental Research Laboratory, NCSR “Demokritos”
Ag. Paraskevi Attikis, Athens 15310 (Greece)

[**] This work was supported by the projects of the ministry of education of the Czech Republic (1M6198959201 and MSM6198959218). We also thank D. Jancik and M. Vujtek for their technical assistance in the microscopy studies.

Supporting Information is available on the WWW under <http://www.small-journal.com> or from the author.

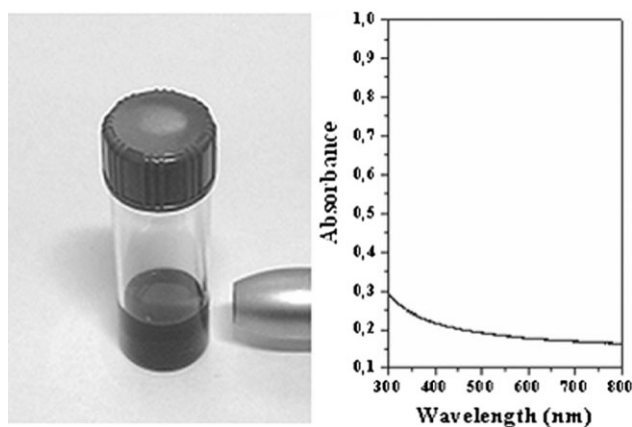


Figure 1. Left: the Tyndall effect is seen here using a laser pointer for the graphite colloidal dispersion in pentafluorobenzonitrile after settling (0.1 mg mL^{-1}). Right: the UV-Vis spectrum of the corresponding dispersion recorded after proper dilution with DMF ($10 \mu\text{g mL}^{-1}$).

(Figure 1). The absorption coefficient measured at 550 nm was $\langle\alpha_{550}\rangle = 1800 \text{ L g}^{-1} \text{ m}^{-1}$. The colloids were clear and stable for at least one month, during which only minor precipitation of solid particulates was observed. Sonication plays an important role in the experimental process by facilitating the solubilization and exfoliation of graphite.^[11a,17] Moreover, the duration of the sonication also affects solubilization with the 1 h span working best for optimal results.^[11a,17] Depending on the solvent, the concentrations of the dispersions after settling were varied between 0.05 and 0.1 mg mL^{-1} , whereas the solubilization yields from 1% to 2%. The performance of each solvent sorted by increasing order was as follows: octafluorotoluene \approx pentafluoropyridine $<$ hexafluorobenzene $<$ pentafluorobenzonitrile. Hence, pentafluorobenzonitrile provided the highest colloidal concentration and solubilization yield (0.1 mg mL^{-1} , 2%) with octafluorotoluene and pentafluoropyridine equally exhibiting the poorest function (0.05 mg mL^{-1} , 1%). Hexafluorobenzene displayed an intermediate efficacy within this series, for example, 0.07 – 0.08 mg mL^{-1} and 1.5% yield. Raman and IR spectroscopy showed practically no oxidization of the as-dispersed graphitic solids (Figure S1 in the Supporting Information).

The mechanism of solubilization most likely involves charge transfer through π – π stacking from the electron-rich carbon layers to the electron-deficient aromatic molecules, the latter containing strong electron-withdrawing fluorine atoms. For instance, the same type of donor–acceptor interactions has been often claimed as the main driving force towards the intercalative derivatization of graphite.^[18–20] Additionally, the solvent–graphene surface matching presents another important aspect that might be responsible for the observed concentration and yield disparities among different solvents.^[11a] The influence of this latter interplay was more striking in the case of pentafluoronitrobenzene, which albeit its strong electron-withdrawing appendages, gave no colloid with graphite. As the single layer concept is by virtue applicable to any other lamellar solid having noncovalent interactions between adjacent layers,^[1,2] we found that treatment of graphite fluoride (CF_x , $x \approx 1$, Aldrich) by the particular solvents afforded colloidal dispersions containing solubilized

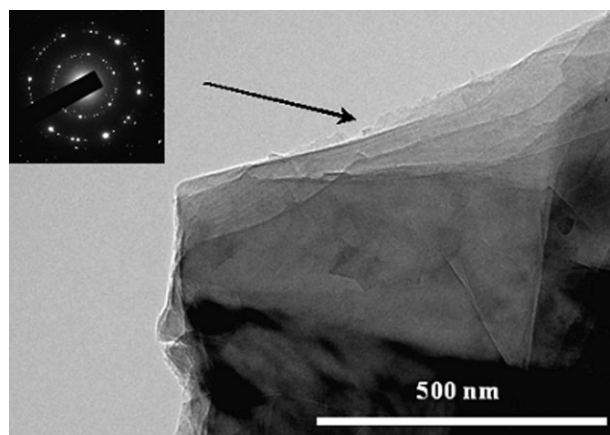


Figure 2. TEM image and selected area electron diffraction (SAED) pattern of an individual graphite flake. The arrow depicts the multilayered structure near the edges of the crystallite.

graphene fluoride single layers instead^[21] (Figure S2 in the Supporting Information). In this case, the observed solubilization can be simply ascribed to the correlated chemical composition of the interacting substances, which in turn confers agreeable surface matching.^[11a]

Transmission electron microscopy (TEM) study of the starting graphite powder (Figure 2) showed thick platy crystallites (lateral size: 0.1 – $5 \mu\text{m}$) possessing a multilayered structure near the edges due to the lamellar registry of several numbers of individual graphene sheets. TEM evaluation of the colloidal dispersions of graphite after drying revealed the presence of transparent and crystalline thin sheets, thus providing a sign of solvent-induced exfoliation (Figure 3). In some cases, the thin sheets could be merely observed by scanning electron microscopy (SEM) as translucent specimens (Figure 3). Multilayered structures with thickness comparable or intermediate (e.g., nanosheets) to that of the pristine crystallites were also noticed, but such objects could be removed by prolonged sedimentation.^[11a] Therefore, the dispersions are essentially an admixture of suspended graphenes (10%–15%), nanosheets, and graphite parti-

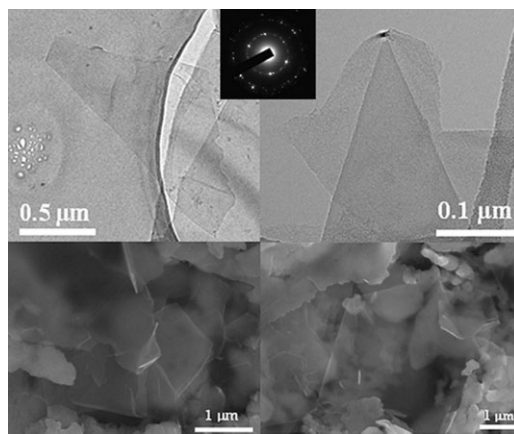


Figure 3. TEM (top) and SEM (bottom) images of some pentafluorobenzonitrile-etched thin sheets. The SAED pattern is included as inset.

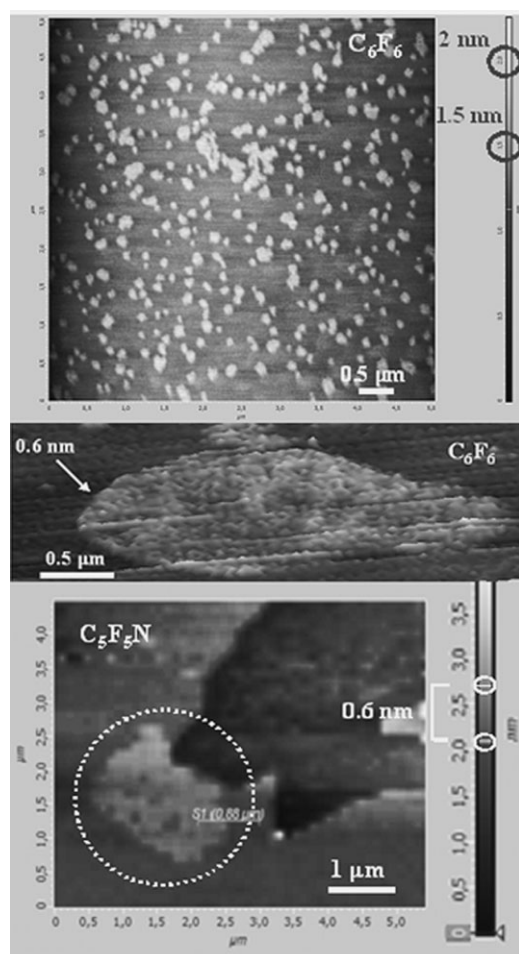


Figure 4. AFM images of some solvent-etched graphenes (the dotted circle at the bottom image marks an individual graphene).

cles.^[11a] The presence of individual graphenes in the as-made samples was confirmed by atomic force microscopy (AFM) (Figure 4). AFM is one of the most direct and precise methods of quantifying the degree of exfoliation to the single-sheet level after dispersing the pristine powder in a solvent. In all instances, we detected several submicrometer- to micrometer-sized nanosheets finely distributed over the mica support. The average thickness of the nanosheets was between 0.5 and 1 nm, as calculated by the height differences through the contrast scale between the surface of the sheets and the mica substrate (Figure 4). Some representative AFM height profiles are given in Figure S3 in the Supporting Information. Such thicknesses are generally consistent with the formation of graphenes (≤ 1 nm).^[22,23] From a technical standpoint, diluted dispersions facilitated our microscopy studies by preventing extensive agglomeration phenomena.

Blank experiments with the analogous hydrocarbon solvents benzene, toluene, nitrobenzene, and pyridine gave access to some noteworthy findings. While graphite was found to form solid suspensions in benzene, toluene, and nitrobenzene that completely settle down after sonication within a day, the situation was markedly different for pyridine (Figure 5). Specifically, after suspending graphite in pyridine by sonication (1 h) and leaving the suspension undisturbed for 5 days in

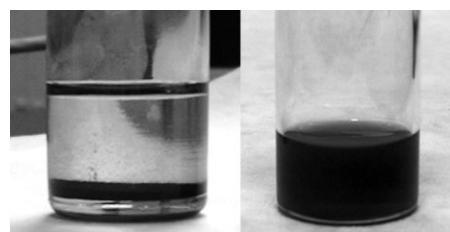


Figure 5. Left: graphite completely settles down after sonication at the bottom of a vial containing benzene, thus leaving the supernatant liquid colorless. Right: partial solubilization of graphite in pyridine by sonication affords a dark colloidal dispersion with concentration 0.3 mg mL^{-1} .

order to gravitationally remove any insoluble particles, a clear deep-black colloidal dispersion was obtained with concentration 0.3 mg mL^{-1} and solubilization yield 6%. The dispersion was stable for about a week, after which complete precipitation occurred. Furthermore, it could be diluted with other solvents^[20] (e.g., DMF) without sedimentation in order to mitigate the unpleasant odor of pyridine and make processing of the colloid much easier. As with the fluorocarbons above, Raman spectroscopy showed no oxidation of the as-dispersed graphitic particles.

The pyridine case suggests that aromatic donors may also exfoliate graphite in the reverse way, that is, charge transfer through π - π stacking from the solvent molecules to the carbon layers (graphite may act either as donor or acceptor, depending on the case). Similar donor-acceptor interactions are quite common in several graphite-intercalated compounds^[18–20] as well as in the pyridine- C_{60} system^[24] and in carbon nanotubes solubilized by certain aromatic amines.^[25] Likewise, molten 2-cyanopyridine (mp: $26\text{--}28^\circ\text{C}$) and benzylamine also provided colloidal dispersions with graphite but aromatic donors like methylpyridines (picolines), aminopicolines, aniline, *N,N*-dimethylaniline, pyrrole, and thiophene did not. Interestingly, the concentration of the benzylamine dispersion reached the impressive value of 1 mg mL^{-1} with marked colloidal stability (>1 month).

TEM analysis of the graphite colloidal dispersion in pyridine after drying also revealed the presence of ultrathin but crystalline sheets (15%–20%), whereas AFM gave conclusive results of the formation of several individual graphenes having 1-nm thickness (Figure 6). Representative AFM height profiles and additional images are provided in Figures S4 and S5 in the Supporting Information. Notably, nearly spherical gold nanoparticles 10–20 nm in diameter were easily deposited on the surface of the as-dispersed graphenes by chemical reduction of a gold compound in solution to afford the corresponding gold-graphene hybrid^[26] (Figure 6).

Aside from the aromatic compounds of the present case study, some non-aromatic solvents that were tested successfully for dispersing graphite included ethyl acetate, vinyl acetate, methyl chloroacetate, 2-methoxyethyl ether, acetylacetone, and *N,N,N',N'*-tetramethylmethylenediamine, which all exhibited remarkable colloidal stabilities and concentrations of $0.2\text{--}0.3 \text{ mg mL}^{-1}$. These common organic solvents also contain strong electron-withdrawing or electron-donating functional groups within their molecular structure as above,

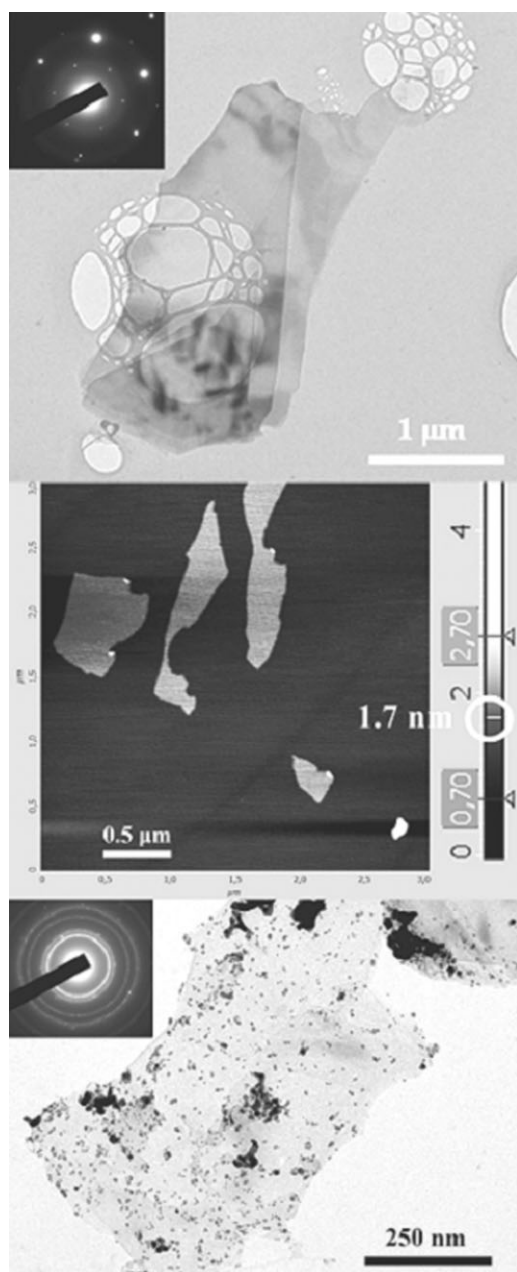


Figure 6. Top: TEM image of a pyridine-etched thin sheet along with its SAED pattern. Middle: AFM image of several pyridine-etched graphenes. Bottom: TEM image and SAED pattern of the gold-graphene hybrid.

however, the solvent–graphene surface matching seems more likely to dominate the solubilization process.^[11a]

In summary, we have introduced a new series of solvents to extract solubilized graphenes from graphite powder. The first set comprises certain electron-deficient perfluorinated aromatic compounds, whereas the second set refers to the aromatic heterocycle of pyridine. Along with these liquids, some other dispersing media have been also listed. Depending on the solvent, graphite can be dispersed at variable concentrations and yields resulting in clear, stable colloids containing solubilized graphenes. We also demonstrated that the as-produced single layers can be easily converted into

gold–graphene hybrids through wet chemistry. The solubility of graphite in such a wide range of solvents is believed to facilitate a broad spectrum of organic reactions with miscible reagents as well as solution processing of several polymer composites.

Experimental Section

The graphite powder was supplied by NUKEM GmbH (Germany). Hexafluorobenzene, octafluorotoluene, pentafluorobenzonitrile, pentafluoronitrobenzene, pentafluoropyridine, and pyridine were all purchased from Aldrich and used as received. IR spectra were taken on a Fourier transform infrared (FTIR) spectrometer (Bruker Equinox 55/S) using KBr pellets. Raman spectra were obtained using an inVia Reflex micro-Raman spectrometer (Renishaw) with a $\times 100$ objective lens and a crystal laser excitation of 514.5 nm operating at 0.1 mW. The optical spectra were recorded on a Shimadzu UV2100 spectrophotometer using quartz cuvettes. TEM was carried out on a JEOL JEM 2010 microscope operated at 200 kV using a holey-carbon-coated copper grid. A FEI INSPECT apparatus operating at 15–30 kV under vacuum was used to record the SEM images of the sheets on Ag substrates. For both TEM and SEM studies, a drop of very dilute dispersion after settling was placed on a substrate and dried at ambient conditions. AFM images were obtained with an AFM (Explorer, ThermoMicroscopes) using a mica substrate in a noncontact mode with silicon tips of the 1650-00 type and resonance frequencies ranging from 180 to 240 kHz. For this purpose, a drop of very dilute dispersion after settling was placed on the mica support and allowed to dry by evaporation at ambient temperature. Generally, dilute dispersions prevented a complete reaggregation of the graphenes.

For the liquid-phase extraction of single layers, graphite fine powder (5 mg) was suspended in a particular aromatic solvent (1 mL) (hexafluorobenzene, octafluorotoluene, pentafluoronitrobenzene, pentafluorobenzonitrile, pentafluoropyridine, or pyridine) by 1 h sonication in an ultrasound bath (135 W) using sealed glass vials. Each suspension was left for 5 days at ambient conditions in order to settle out any insoluble particles and the supernatant clear colloids were carefully collected for further microscopy characterization. The concentration of a given dispersion was measured quantitatively by filtering a large volume of the colloid through a pre-weighed filter (Millipore HVLP 0.45 μm). After the solvent had been completely removed, the filter with the solid residue on it was dried and re-weighed using a high precision balance. The solubilization yields, expressed as percentages, were calculated for each case from the soluble content in mg per 1 mL solvent divided by the initially added amount of graphite in 1 mL solvent (5 mg).

To prepare the gold–graphene hybrid, a solution of $\text{HAuCl}_4 \cdot 3\text{H}_2\text{O}$ (0.5 mg) in DMF (1 mL) was added in the graphite colloidal dispersion in pyridine (10 mL, 0.1 mg mL^{-1}) followed by reduction with NaBH_4 (2 mg) under vigorous stirring. The resulting precipitate was centrifuged, washed with ethanol, and air-dried.

Keywords:

graphene · graphite · liquid-phase exfoliation · solubilization · solvent effects

- [1] a) K. S. Novoselov, A. K. Geim, S. V. Morozov, D. Jiang, Y. Zhang, S. V. Dubonos, I. V. Grigorieva, A. A. Firsov, *Science* **2004**, *306*, 666–669; b) K. S. Novoselov, D. Jiang, F. Schedin, T. J. Booth, V. V. Khotkevich, S. V. Morozov, A. K. Geim, *Proc. Natl. Acad. Sci. USA* **2005**, *102*, 10451–10453; c) A. K. Geim, K. S. Novoselov, *Nat. Mater.* **2007**, *6*, 183–191.
- [2] a) M. I. Katsnelson, *Mater. Today* **2007**, *10*, 20–27; b) J. Wood, *Mater. Today* **2007**, *10*, 1.
- [3] a) C. Berger, Z. Song, X. Li, X. Wu, N. Brown, C. Naud, D. Mayou, T. Li, J. Hass, A. N. Marchenkov, E. H. Conrad, P. N. First, W. A. de Heer, *Science* **2006**, *312*, 1191–1196; b) H. Huang, W. Chen, S. Chen, A. T. S. Wee, *ACS Nano* **2008**, *2*, 2513–2518.
- [4] a) S. Stankovich, D. A. Dikin, G. H. B. Dommett, K. M. Kohlhaas, E. J. Zimney, E. A. Stach, R. D. Piner, S.-B. T. Nguyen, R. S. Ruoff, *Nature* **2006**, *442*, 282–286; b) D. A. Dikin, S. Stankovich, E. J. Zimney, R. D. Piner, G. H. B. Dommett, G. Evmenenko, S.-B. T. Nguyen, R. S. Ruoff, *Nature* **2007**, *448*, 457–460.
- [5] a) D. Li, M. B. Müller, S. Gilje, R. B. Kaner, G. G. Wallace, *Nat. Nanotechnol.* **2008**, *3*, 101–105; b) V. C. Tung, M. J. Allen, Y. Yang, R. B. Kaner, *Nat. Nanotechnol.* **2009**, *4*, 25–29.
- [6] R. Ruoff, *Nat. Nanotechnol.* **2008**, *3*, 10–11.
- [7] a) X. Li, X. Wang, L. Zhang, S. Lee, H. Dai, *Science* **2008**, *319*, 1229–1232; b) X. Li, G. Zhang, X. Bai, X. Sun, X. Wang, E. Wang, H. Dai, *Nat. Nanotechnol.* **2008**, *3*, 538–542.
- [8] J. Zhu, *Nat. Nanotechnol.* **2008**, *3*, 528–529.
- [9] a) L. Zhi, K. Müllen, *J. Mater. Chem.* **2008**, *18*, 1472–1484; b) M. Choucair, P. Thordarson, J. A. Stride, *Nat. Nanotechnol.* **2009**, *4*, 30–33.
- [10] a) P. W. Sutter, J.-I. Flege, E. A. Sutter, *Nat. Mater.* **2008**, *7*, 406–411; b) Y. S. Dedkov, M. Fonin, U. Rüdiger, C. Laubschat, *Phys. Rev. Lett.* **2008**, *100*, 107602(4); c) A. T. N'Diaye, J. Coraux, T. N. Plasa, C. Busse, T. Michely, *New J. Phys.* **2008**, *10*, 043033(16).
- [11] a) Y. Hernandez, V. Nicolosi, M. Lotya, F. M. Blighe, Z. Sun, S. De, I. T. McGovern, B. Holland, M. Byrne, Y. K. Guñko, J. J. Boland, P. Niraj, G. Duesberg, S. Krishnamurthy, R. Goodhue, J. Hutchison, V. Scardaci, A. C. Ferrari, J. N. Coleman, *Nat. Nanotechnol.* **2008**, *3*, 563–568; b) C. Vallés, C. Drummond, H. Saadaoui, C. A. Furtado, M. He, O. Roubeau, L. Ortolani, M. Monthieux, A. Pénicaud, *J. Am. Chem. Soc.* **2008**, *130*, 15802–15804.
- [12] a) S. Niyogi, E. Bekyarova, M. E. Itkis, J. L. McWilliams, M. A. Hamon, R. C. Haddon, *J. Am. Chem. Soc.* **2006**, *128*, 7720–7721; b) E. Bekyarova, M. E. Itkis, P. Ramesh, C. Berger, M. Sprinkle, W. A. de Heer, R. C. Haddon, *J. Am. Chem. Soc.* **2009**, *131*, 1336–1337.
- [13] J. R. Lomeda, C. D. Doyle, D. V. Kosynkin, W.-F. Hwang, J. M. Tour, *J. Am. Chem. Soc.* **2008**, *130*, 16201–16206.
- [14] K. Züchner, T. J. Richardson, O. Glemser, N. Bartlett, *Angew. Chem. Int. Ed.* **1980**, *19*, 944–945.
- [15] A. V. Okotrub, V. D. Yumatov, L. N. Mazalov, G. G. Furin, V. V. Murakhtanov, L. G. Bulusheva, *J. Struct. Chem.* **1989**, *29*, 720–727.
- [16] J. Langer, I. Dąbkowska, Y. Zhang, E. Illenberger, *Phys. Chem. Chem. Phys.* **2008**, *10*, 1523–1531.
- [17] a) S.-H. Jeong, O.-J. Lee, K.-H. Lee, S.-H. Oh, C.-G. Park, *Chem. Mater.* **2002**, *14*, 1859–1862; b) L. M. Viculis, J. J. Mack, R. B. Kaner, *Science* **2003**, *299*, 1361.
- [18] M. Inagaki, *New Carbons: Control of Structure and Functions*, Elsevier, Oxford **2000**.
- [19] M. Inagaki, *J. Mater. Res.* **1989**, *4*, 1560–1568.
- [20] R. Hao, W. Qian, L. Zhang, Y. Hou, *Chem. Commun.* **2008**, 6576–6578.
- [21] K. A. Worsley, P. Ramesh, S. K. Mandal, S. Niyogi, M. E. Itkis, R. C. Haddon, *Chem. Phys. Lett.* **2007**, *445*, 51–56.
- [22] P. Nemes-Incze, Z. Osváth, K. Kamarás, L. P. Biró, *Carbon* **2008**, *46*, 1435–1442.
- [23] I. Jung, D. A. Dikin, R. D. Piner, R. S. Ruoff, *Nano Lett.* **2008**, *8*, 4283–4287.
- [24] F. Zhang, Y. Fang, *J. Phys. Chem. B* **2006**, *110*, 9022–9026.
- [25] Y. Sun, S. R. Wilson, D. I. Schuster, *J. Am. Chem. Soc.* **2001**, *123*, 5348–5349.
- [26] R. Muszynski, B. Seger, P. V. Kamat, *J. Phys. Chem. C* **2008**, *112*, 5263–5266.

Received: February 9, 2009
Revised: March 17, 2009
Published online: April 30, 2009